ARTICLE

https://doi.org/10.1038/s41586-019-1155-x

^{78}Ni revealed as a doubly magic stronghold against nuclear deformation

R. Taniuchi[1,2], C. Santamaria[2,3], P. Doornenbal[2*], A. Obertelli[2,3,4], K. Yoneda[2], G. Authelet[3], H. Baba[2], D. Calvet[3], F. Château[3], A. Corsi[3], A. Delbart[3], J.-M. Gheller[3], A. Gillibert[3], J. D. Holt[5], T. Isobe[2], V. Lapoux[3], M. Matsushita[6], J. Menéndez[6], S. Momiyama[1,2], T. Motobayashi[2], M. Niikura[1], F. Nowacki[7], K. Ogata[8,9], H. Otsu[2], T. Otsuka[1,2,6], C. Péron[3], S. Péru[10], A. Peyaud[3], E. C. Pollacco[3], A. Poves[11], J.-Y. Roussé[3], H. Sakurai[1,2], A. Schwenk[4,12,13], Y. Shiga[2,14], J. Simonis[4,12,15], S. R. Stroberg[5,16], S. Takeuchi[2], Y. Tsunoda[6], T. Uesaka[2], H. Wang[2], F. Browne[17], L. X. Chung[18], Z. Dombradi[19], S. Franchoo[20], F. Giacoppo[21], A. Gottardo[20], K. Hadyńska-Klęk[21], Z. Korkulu[19], S. Koyama[1,2], Y. Kubota[2,6], J. Lee[22], M. Lettmann[4], C. Louchart[4], R. Lozeva[7,23], K. Matsui[1,2], T. Miyazaki[1,2], S. Nishimura[2], L. Olivier[20], S. Ota[6], Z. Patel[24], E. Şahin[21], C. Shand[24], P.-A. Söderström[2], I. Stefan[20], D. Steppenbeck[6], T. Sumikama[25], D. Suzuki[20], Z. Vajta[19], V. Werner[4], J. Wu[2,26] & Z. Y. Xu[22]

Nuclear magic numbers correspond to fully occupied energy shells of protons or neutrons inside atomic nuclei. Doubly magic nuclei, with magic numbers for both protons and neutrons, are spherical and extremely rare across the nuclear landscape. Although the sequence of magic numbers is well established for stable nuclei, experimental evidence has revealed modifications for nuclei with a large asymmetry between proton and neutron numbers. Here we provide a spectroscopic study of the doubly magic nucleus ^{78}Ni, which contains fourteen neutrons more than the heaviest stable nickel isotope. We provide direct evidence of its doubly magic nature, which is also predicted by ab initio calculations based on chiral effective-field theory interactions and the quasi-particle random-phase approximation. Our results also indicate the breakdown of the neutron magic number 50 and proton magic number 28 beyond this stronghold, caused by a competing deformed structure. State-of-the-art phenomenological shell-model calculations reproduce this shape coexistence, predicting a rapid transition from spherical to deformed ground states, with ^{78}Ni as the turning point.

Outline of this work

- First spectroscopy on ^{78}Ni has been performed at RIBF, RIKEN.
- Excited states of ^{78}Ni were obtained by combination of the two key detectors; DALI2 γ-ray spectrometer and MINOS liquid hydrogen system.
- Doubly shell-closure of ^{78}Ni has been confirmed.
- At the same time, emergence of shape-coexistence nature in ^{78}Ni has been suggested, resulting in the possible quenching of neutron- and proton-shell gaps beyond this anchor point.

News and Views in the same issue

NUCLEAR PHYSICS

A doubly magic nucleus that has two faces

The neutron-rich nickel nucleus ^{78}Ni is difficult to excite and, once excited, has competing spherical and deformed shapes. These intriguing properties make ^{78}Ni a valuable testing ground for nuclear theory. SEE ARTICLE P.53

GAUTE HAGEN & THOMAS PAPENBROCK

Nature **569**, 49-50 (2019)

https://doi.org/10.1038/d41586-019-01321-4

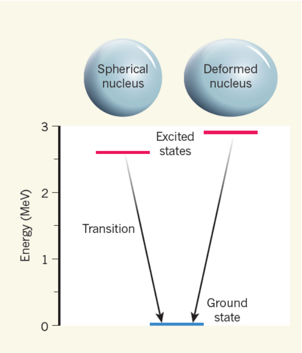

Figure 1 | Properties of the nickel nucleus ^{78}Ni. Taniuchi *et al.*[1] report transitions of ^{78}Ni between excited states and the ground state. An excited

RIKEN’s top page

Table of Contents

Table of Contents

Nucleus: a quantum many-body system

- A picture of nuclear structure: nucleons in single particle states
- Large gaps at 2, 8, 20, 28, 50,· · · , reproduced by a spin-orbit interaction in a Woods-Saxon type potential
- Magic numbers are the numbers of proton and neutron at shell-closure
- 28, 50,.. are the numbers induced by spin-orbit splittings

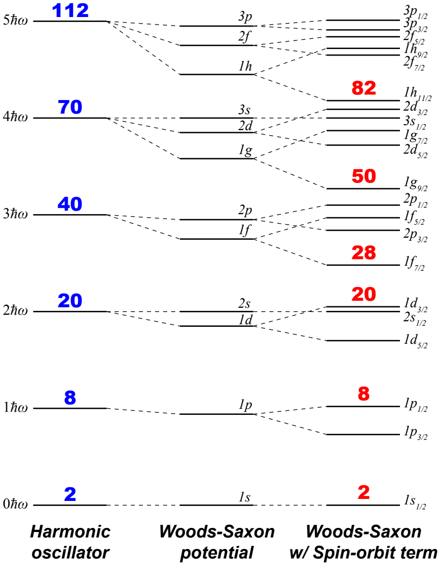

How to determine the shell closures?

- Systematic trend of mass difference is a direct indication of the ground state property.
- Two-neutron separation energy, S_{2n}, are shown. Sudden drops above $N = 50$ gap are evident.
- It's hard to reach exotic region.

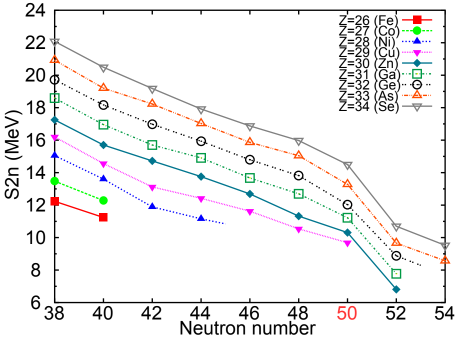

How to determine the shell closures?

- Systematic trend of mass difference is a direct indication of the ground state property.
- Two-neutron separation energy, S_{2n}, are shown. Sudden drops above $N = 50$ gap are evident.
- It's hard to reach exotic region.

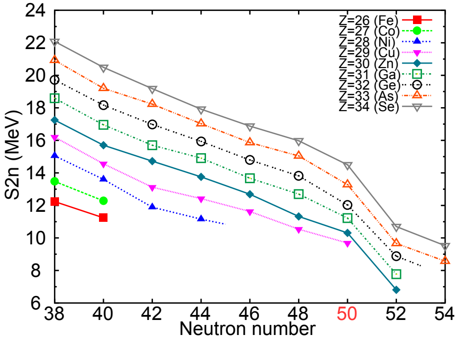

- Instead, the excitation energy works as a good indicator of shell closure and single particle energies.
- The energy of first 2^+ state of even-even nuclei is rather commonly used for a first clue of shell-closure.

$E(2^+_1)$ systematics among the nuclear chart

- The energy $E(2^+)$ is a good indicator of the shell closure.
- ^{78}Ni is the only candidate of the unobserved neutron-rich particle-bound doubly magic nuclei.
- Aim of this work: First γ-ray spectroscopy of doubly magic ^{78}Ni.

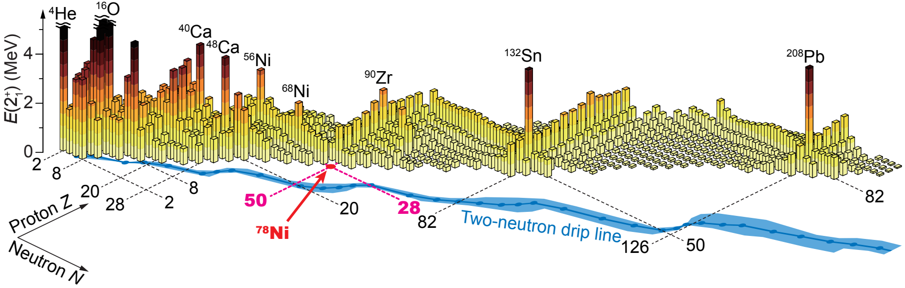

(Evaluation of the drip line from J. Erler *et al.*, Nature **486**, 509-512 (2012))

“Magic numbers” are not universal

Emergence of a new magic numbers

Appearance of shell-closure along calcium isotopes in ^{52,54}Ca was confirmed by high excitation energies $E(2^+)$. This indicates new magic numbers: $N = 32, 34$.

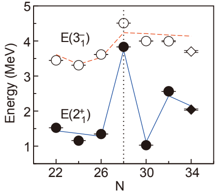

(Figure from D. Steppenbeck *et al.*, Nature **502**, 207-210 (2013))

Disappearance of magic number

Low excitation energy of ^{42}Si indicates the $N = 28$ shell closure has been collapsed in much less proton nuclei.

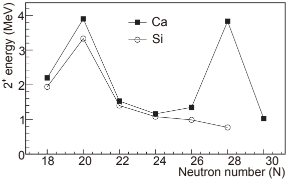

(Figure from B. Bastin *et al.*, Phys. Rev. Lett. **99**, 022503 (2007))

What is the driving force of the “rearrangement”?

- Tensor term was pointed out as a major reason for modifying these shell gaps. It works between protons and neutrons as reducing the spin-orbit splitting.
- Toward ^{78}Ni, the $Z = 28$ gap are expected to be reduced by filling neutrons in $g_{9/2}$ shell up to $N = 50$.
- While, the $N = 50$ gap is assumed to be collapsed in less proton nuclei $Z < 28$, below ^{78}Ni.

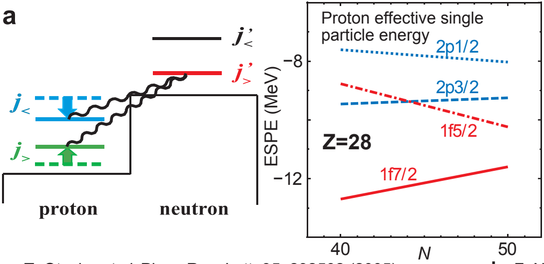

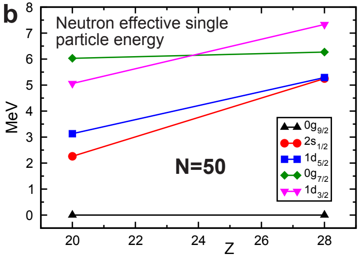

a: T. Otsuka *et al.* Phys. Rev. Lett. **95**, 232502 (2005)

b: F. Nowacki *et al.* Phys. Rev. Lett. **117**, 272501 (2016)

Experimental studies of ^{78}Ni

Benchmarking the nuclear structure in the most neutron-rich doubly magic nuclei

- First production at GSI: 3 counts in 5.5 days [1].
- First β-decay halflife $T_{1/2}$ measurement at NSCL: 11 counts in 4.3 days [2].
- Halflife measurement at RIBF: 4000 counts in 7.5 days [3].
  $\rightarrow$ Indication of magicity

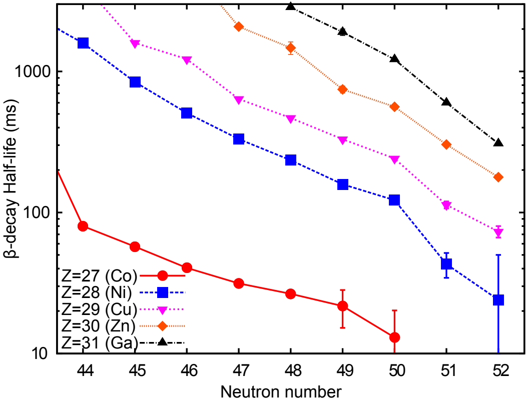

[1] Ch. Engelmann *et al.*, Z. Phys. A **352**, 351-352 (1995)
[2] P.T. Hosmer *et al.*, Phys. Rev. Lett. **94**, 112501 (2005)
[3] Z.Y. Xu *et al.*, Phys. Rev. Lett. **113**, 032505 (2014)

Theoretical predictions along $Z = 28$ chain

- Most theoretical calculations predict the $E(2^+)$ at around 3 MeV, suggesting the doubly shell-closure of ^{78}Ni.

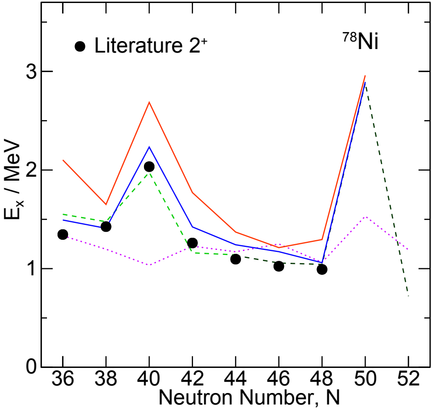

A3DA-m solid: 2^+, dashed 4^+
Monte Carlo shell model (Tokyo)
pf-$g_{9/2}$-$d_{5/2}$ orbitals for both proton and neutron
Y. Tsunoda *et al.*, Phys. Rev. C **89**, 031301(R) (2014)

LNPS
Large scale shell model (Strasbourg)
pf (proton) and $f_{5/2}$-$p_{1/2,3/2}$-$d_{5/2}$ orbitals (neutron)
S. Lenzi *et al.*, Phys. Rev. C **82**, 054301 (2010)

PFSDG-U
Large scale shell model (Strasbourg)
pf (proton) and *sdg* (neutron)
F. Nowacki *et al.*, Phys. Rev. Lett. **117**, 272501 (2016)

QRPA
Beyond mean-field calculation (S. Péru)
based on finite-range Gogny D1S interaction
S. Péru and M. Martini, EPJA **50**, 88 (2014)

5DCH (5-dimensional collective hamiltonian)
J.P. Delaroche *et al.*, Phys. Rev. C **81**, 014303 (2010)

Shape coexistence in ^{78}Ni

- Potential energy surface in the β-γ plane illustrates axial and triaxial quadrupole deformation
- Respective large scale shell model calculatons indicate controversial results

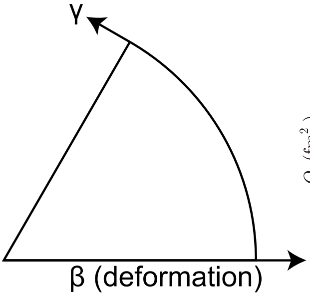

A3DA-m

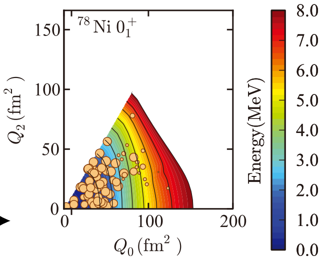

PFSDG-U

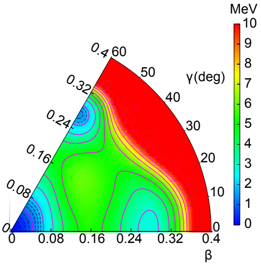

A3DA-m	Monte Carlo shell model (Tokyo): *pf*-$g_{9/2}$-$d_{5/2}$ orbitals for both proton and neutron Y. Tsunoda et al., Phys. Rev. C **89**, 031301(R) (2014)
PFSDG-U	Large scale shell model (Strasbourg): *pf* (proton) and *sdg* (neutron) F. Nowacki *et al.*, Phys. Rev. Lett. **117**, 272501 (2016)

Other studies around ^{78}Ni

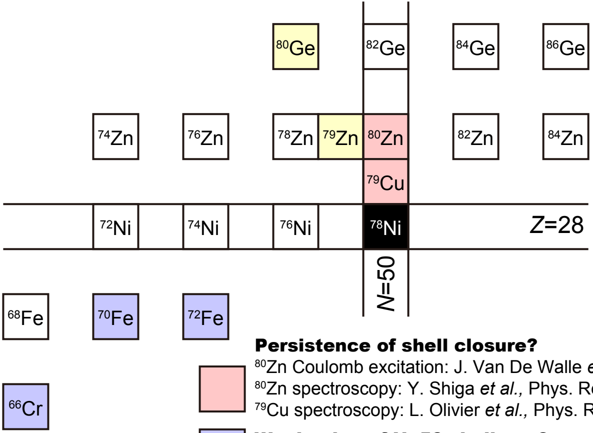

Persistence of shell closure?

^{80}Zn Coulomb excitation: J. Van De Walle *et al.,* Phys. Rev. Lett **99**, 142501 (2007)
^{80}Zn spectroscopy: Y. Shiga *et al.,* Phys. Rev. C **93**, 024320(2016)
^{79}Cu spectroscopy: L. Olivier *et al.,* Phys. Rev. Lett. **119**, 192501(2017)

Weakening of N=50 shell gap?

E(2+) of ^{66}Cr, ^{70,72}Fe: C. Santamaria *et al.,* Phys. Rev. Lett. **115**, 192501 (2015)

Shape coexistence emerges in 78Ni?

β-delayed conversion electron of ^{80}Ge: A. Gottardo *et al.,* Phys. Rev. Lett **116**, 182501(2016)
Isomer shift of ^{79}Zn: X.F. Yang *et al.,* Phys. Rev. Lett. **116**, 182502(2016)

Table of Contents

Two-step reaction to populate excited states of ^{78}Ni

- Primary ^{238}U with 345 MeV/u at an average intensity of **13 pnA**
- Secondary beam from in-flight fission of ^{238}U collected by BigRIPS
- A secondary target and a γ-ray spectrometer were installed in the midst of magnetic spectrometers, F8
- $^{79}\mathrm{Cu}(p,2p)^{78}\mathrm{Ni}$ and $^{80}\mathrm{Zn}(p,3p)^{78}\mathrm{Ni}$ reactions

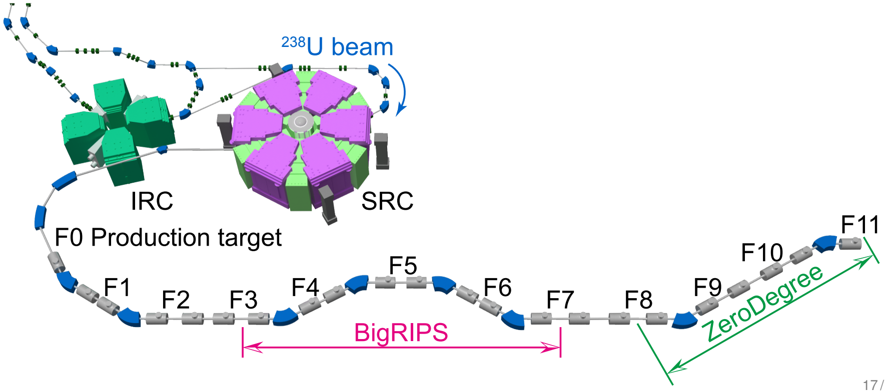

$B\rho - \Delta E -$TOF method applied for PID

Observations

- Velocity β: Deduced from TOF (Time of flight)

$$\beta = \frac{L}{c} \cdot \frac{1}{TOF}.$$

- Atomic number Z: Deduced from β and energy loss ΔE

$$-\frac{dE}{dx} = \frac{4\pi}{m_e c^2} \cdot \frac{Z^2}{\beta^2} \cdot \left(\frac{e^2}{4\pi\varepsilon_0}\right)^2 \cdot n \left[\ln\left(\frac{2m_e c^2\beta^2}{I(1-\beta^2)}\right) - \beta^2\right].$$

- Mass-to-charge ratio A/Q: From β and magnetic rigidity $B\rho$

$$\gamma m \frac{v^2}{\rho} = QvB, \qquad B\rho = \frac{\gamma m v}{Q} = \frac{\beta\gamma c m_u}{e} \cdot \frac{A}{Q}.$$

Beamline detectors for particle identification

Detectors

- TOF: Timings between plastic scintillators
  location: both ends of each spectrometer (F3, F7, F8, and F11)
- ΔE: Energy loss was obtained by MUSIC (multi-sampling ionization chamber)
  location: end of each spectrometer (F7 and F11)
- $B\rho$: Positions and angles were obtained by PPAC (position-sensitive Parallel Plate Avalanche Counters)
  location: dispersive (F5, F9) and achromatic (F3, F7, F8, and F11) foci

Obtained particle identification plots

PID in upstream (BigRIPS)

^{79}Cu: 5.2 particles/s

^{80}Zn: 290 particles/s

PID in downstream (ZeroDegree)

^{79}Cu$(p, 2p)^{78}$Ni: 937 evts

^{80}Zn$(p, 3p)^{78}$Ni: 815 evts

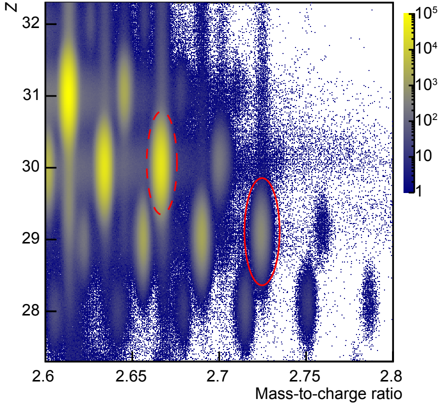

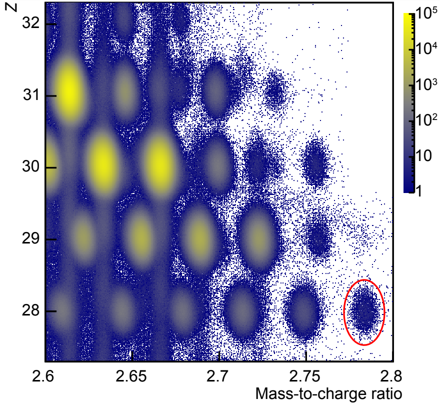

Secondary reaction target and γ-ray detector array

- Thick liquid hydrogen target (MINOS): Tracks of the recoil protons were obtained to reconstuct the reaction vertices. $\Delta x \sim 5$ mm.
- High-efficiency scintillator array (DALI2): Intrinsic resolution and efficiency were 10% and 20% for 1 MeV γ-ray from moving system.

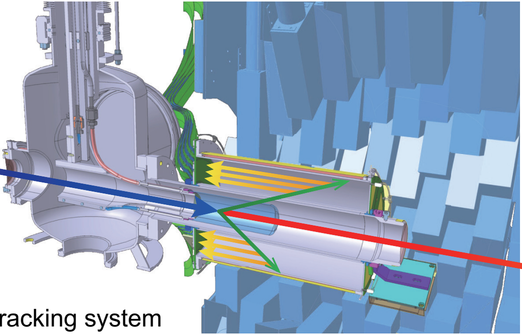

Doppler broadening in in-beam γ-ray spectroscopy

Uncertainty of the γ-ray energy from Doppler broadening should be taken into accont to gain the luminosity by employing thick secondary target.

$$\frac{E_\gamma}{E_{\gamma 0}} = \frac{\sqrt{1-\beta^2}}{1-\beta\cos\theta_\gamma}, \qquad \delta^2_{\mathrm{tot.}} = \left(\frac{\Delta E_{\gamma 0}}{E_{\gamma 0}}\right)^2 = \delta^2_\theta + \delta^2_\beta + \delta^2_{\mathrm{intr.}}.$$

10-cm liquid hydrogen without vertex reconstruction

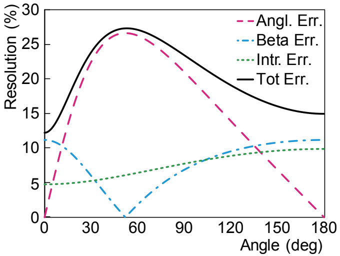

10-cm liquid hydrogen with vertex reconstruction

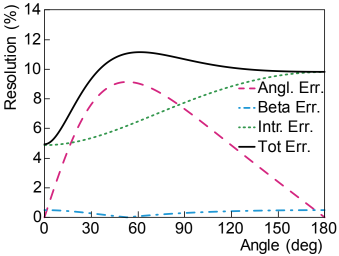

Vertex image reconstructed by MINOS

- Determine the vertex position by two protons and beam trajectory

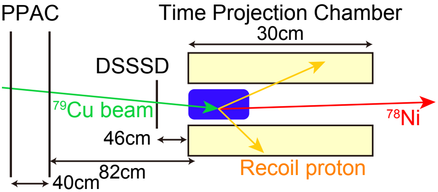

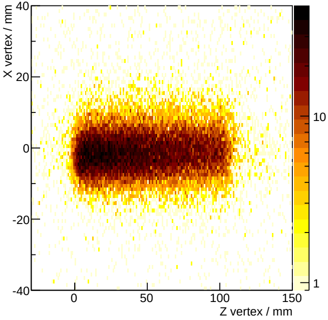

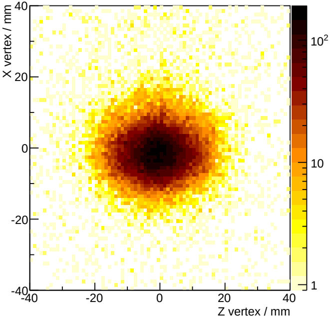

Spectra of ^{80}Zn via $(p, 2p)$ and $(p, 3p)$ reactions

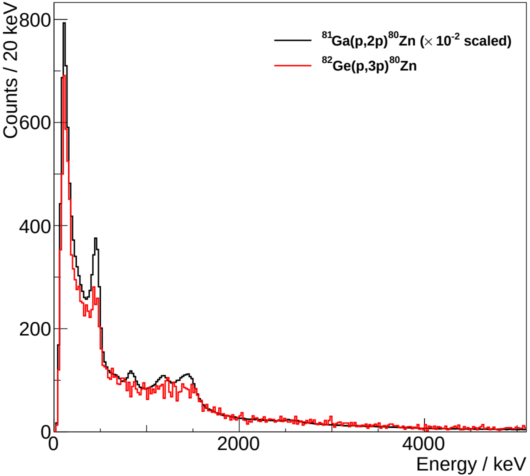

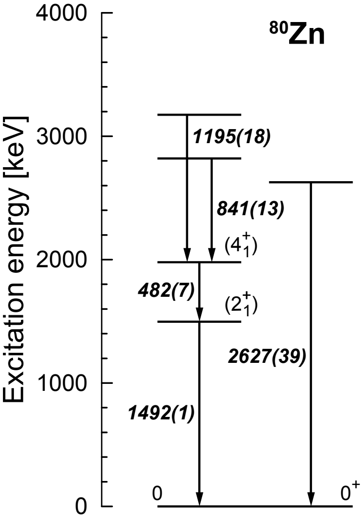

Spectra of ^{79}Cu via (p, 2p) and (p, 3p) reactions

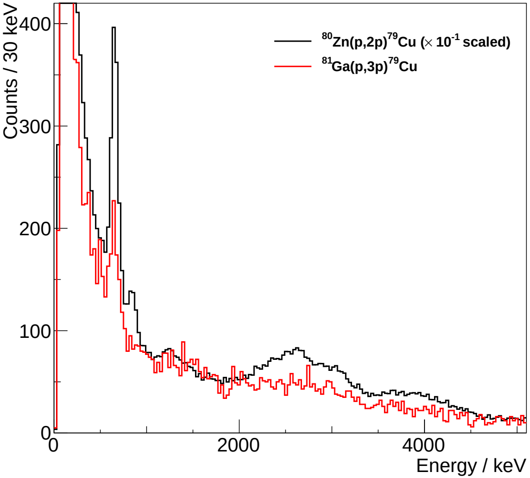

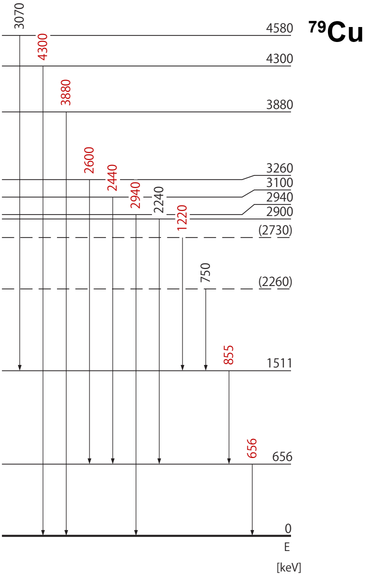

Table of Contents

Different γ-ray populations in respective reactions

While a strong γ-ray population at 2600 keV can be seen in the $(p, 2p)$ reaction, another 2900-keV transition is observed in the $(p, 3p)$ channel.

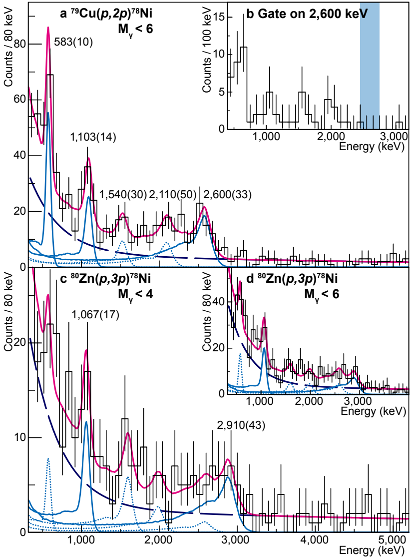

Strategy for analyzing the γ-ray spectra of respective reaction channels

- Analyze spectrum of each reaction channel, $(p, 2p)$ and $(p, 3p)$, individually.
- Energy determination of the peaks: maximum likelihood, using multi-dimensional probability function.
- Significance levels: *p*-test deduced by likelihood-ratio.
- Reconstruction of energy levels: intensity relationship and γ-γ analysis.

The $^{79}Cu(p, 2p)^{78}Ni$ channel

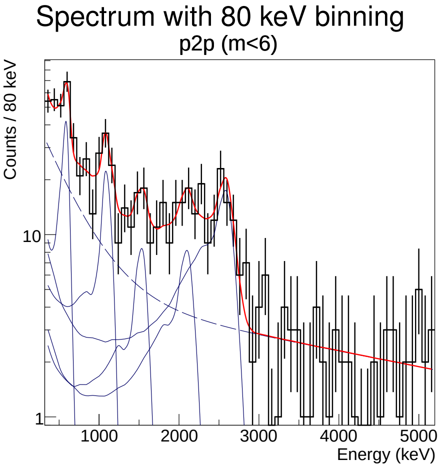

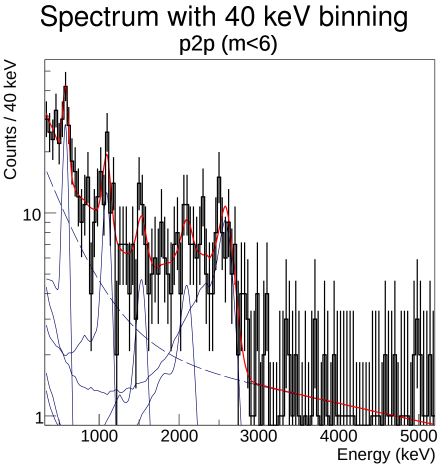

The $^{79}Cu(p,2p)^{78}Ni$ channel

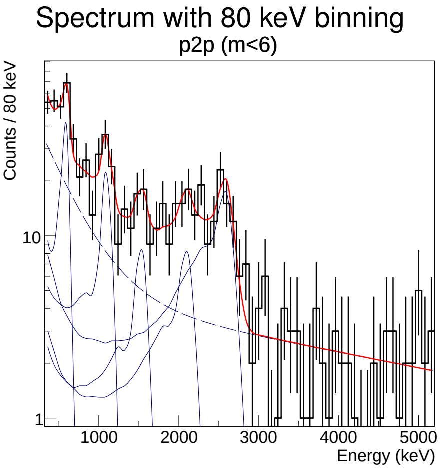

- Maximum likelihood with 5 response functions and a double-exponential function

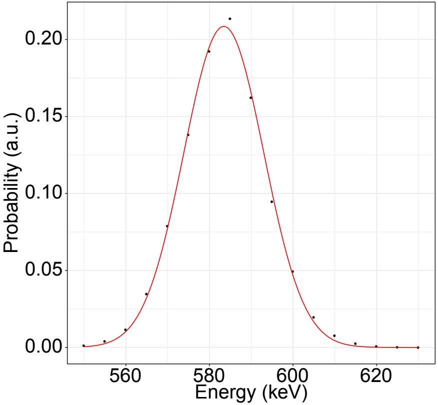

The ^{79}Cu(p, 2p)^{78}Ni channel

Spectrum with 80 keV binning

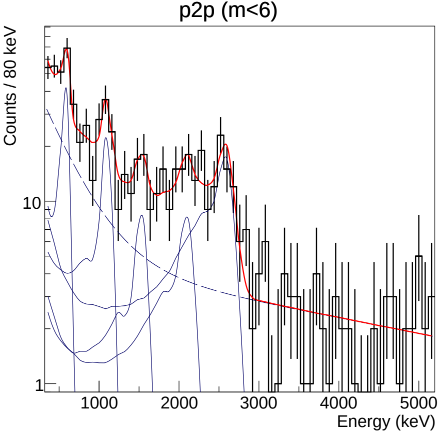

- Result with 1 s.d. error of E_γ and relative intensity I_{rel}
- Significance levels were deduced from p-test

E_γ (keV)	I_{rel} (%)	S. L.
583(10)	49(11)	5.3
1103(14)	49(12)	4.3
1540(25)	28(11)	2.6
2110(48)	33(13)	2.9
2600(33)	100(15)	7.5

The ^{79}Cu(p, 2p)^{78}Ni channel

Spectrum with 80 keV binning

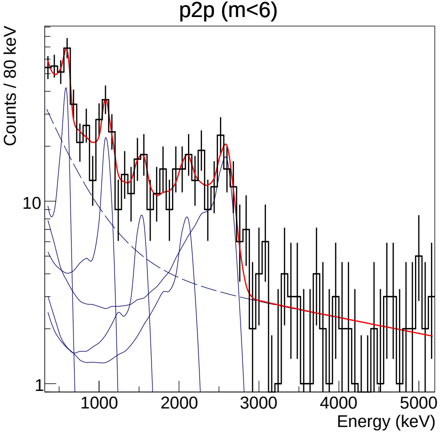

- Result with 1 s.d. error of E_γ and relative intensity I_{rel}
- Significance levels were deduced from p-test

E_γ (keV)	I_{rel} (%)	S. L.
583(10)	49(11)	5.3
1103(14)	49(12)	4.3
1540(25)	28(11)	2.6
2110(48)	33(13)	2.9
2600(33)	100(15)	7.5
2910(43)	—	1.2

γ-γ coincidence analysis

All low-lying transitions are feeding the 2600 keV state

- γ-γ coincidence spectrum after gating with 2600 keV transition
- All four low-lying states are in coincidence.
- No background events were subtracted

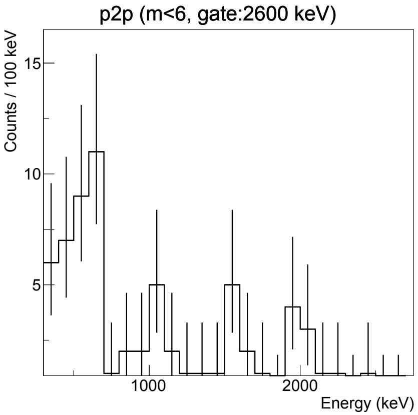

γ-γ coincidence analysis

No coincidence between 583 keV and 1103 keV

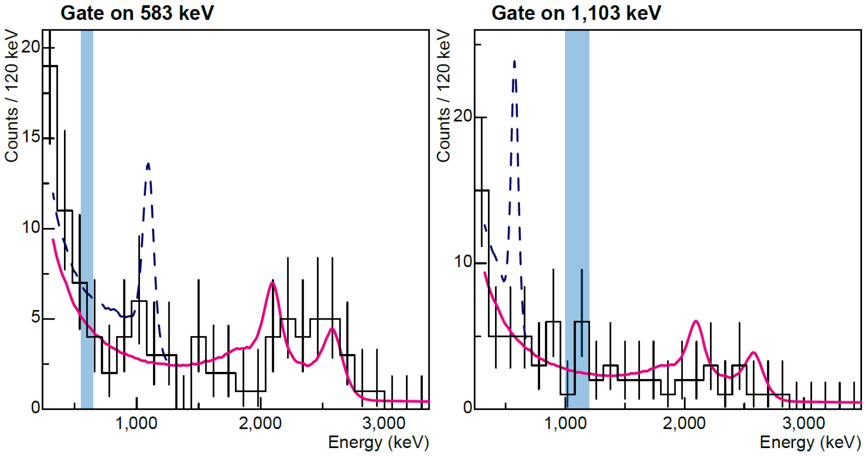

The ^{80}Zn$(p, 3p)^{78}$Ni channel

High lying transition at 2900 keV

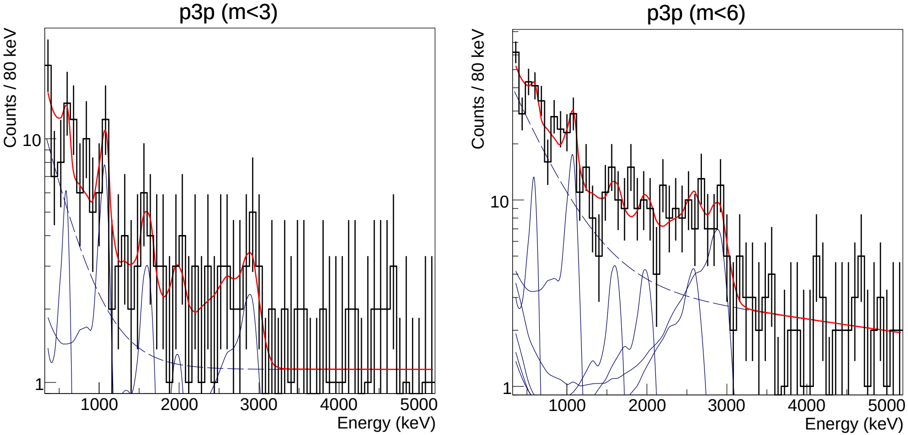

The ^{80}Zn(p, 3p)^{78}Ni channel

High lying transition at 2900 keV

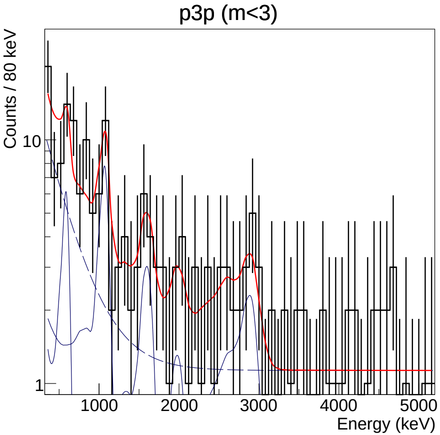

- A transition at 2910(43) keV was found, which was not seen in the (p, 2p) reaction
- Enhancement at lower γ-ray multiplicity condition and the large intensity are seen

E_γ (keV)	I_{rel} (%)	S. L.
581(16)	46(19)	1.8
1067(17)	84(26)	3.5
2710(200)	48(30)	1.4
2910(43)	100(29)	3.7

Evolution of I_{rel} and significance levels with γ-ray multiplicity

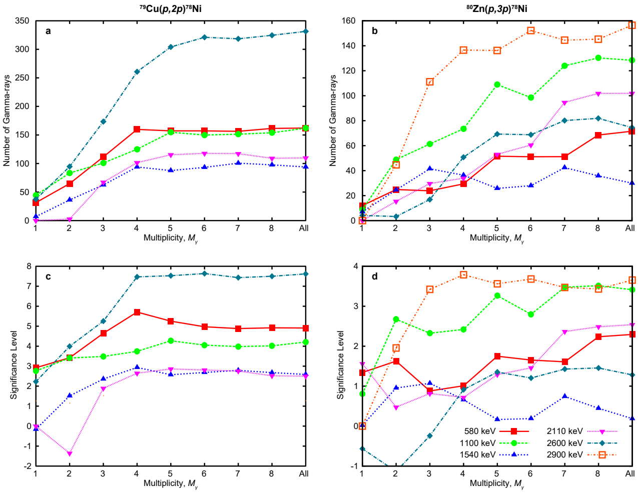

Obtained level scheme of ^{78}Ni

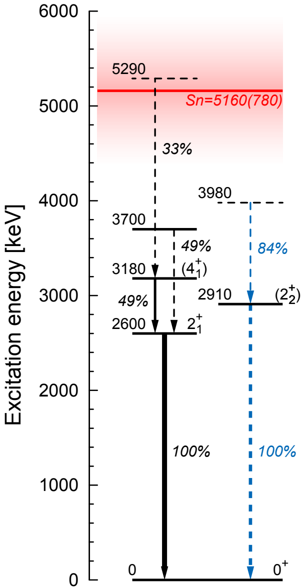

- Black and blue transitions were observed in the $(p, 2p)$ and $(p, 3p)$ reactions, respectively.
- Solid line: Significance level $\geq 5\sigma$
- The most strong transitions at 2600 keV and 2900 keV in respective reactions are tentatively assigned as 2^+ states feeding the ground state directly.
- The state at 3180 keV is tentatively assigned as 4^+ state.

Table of Contents

2_1^+, 4_1^+: Doubly magic nature in ^{78}Ni is preserved

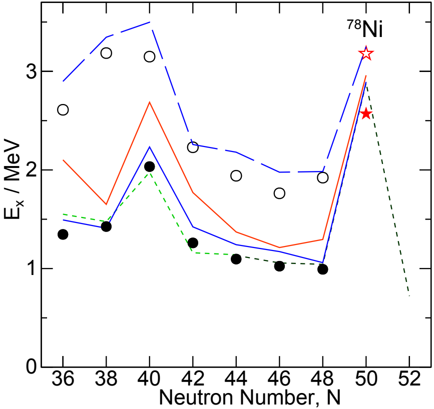

- ● Literature 2^+ ○ Literature 4^+
- ★ This work 2^+ ☆ This work 4^+

— A3DA-m solid: 2^+, dashed 4^+
Monte Carlo shell model (Tokyo)
pf-$g_{9/2}$-$d_{5/2}$ orbitals for both proton and neutron
Y. Tsunoda *et al.,* Phys. Rev. C **89**, 031301(R) (2014)

- - - LNPS
Large scale shell model (Strasbourg)
pf (proton) and $f_{5/2}$-$p_{1/2,3/2}$-$d_{5/2}$ orbitals (neutron)
S. Lenzi *et al.,* Phys. Rev. C **82**, 054301 (2010)

- - - PFSDG-U
Large scale shell model (Strasbourg)
pf (proton) and *sdg* (neutron)
F. Nowacki *et al.*, Phys. Rev. Lett. **117**, 272501 (2016)

— QRPA
Beyond mean-field calculation (S. Péru)
based on finite-range Gogny interaction
S. Péru and M. Martini, EPJA **50**, 88 (2014)

What can be the origin of 2_2^+ state?

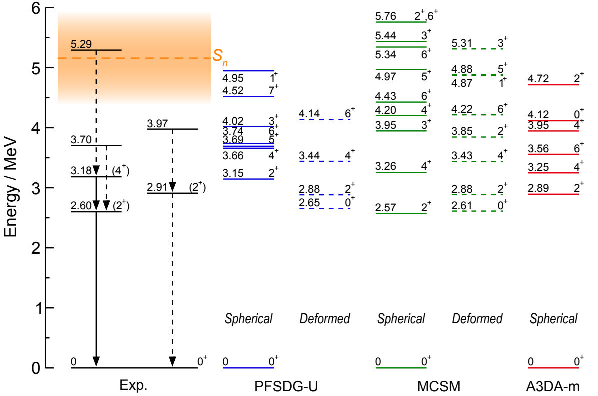

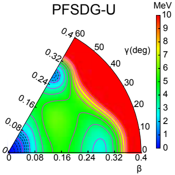

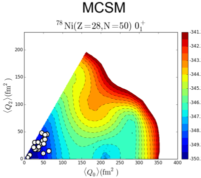

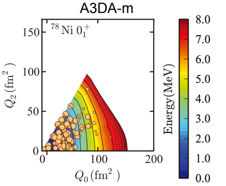

PFSDG-U	Large scale shell model (Strasbourg): *pf* (proton) and *sdg* (neutron) F. Nowacki *et al.*, Phys. Rev. Lett. **117**, 272501 (2016)
A3DA-m	Monte Carlo shell model (Tokyo): *pf*-$g_{9/2}$-$d_{5/2}$ orbitals for both proton and neutron Y. Tsunoda *et al.*, Phys. Rev. C **89**, 031301(R) (2014)
MCSM	New Monte Carlo shell model (Tokyo): *pfgds* shells for both proton and neutron Y. Tsunoda *et al.*, Private communication

Average numbers of particle-hole (p-h) excitations

Comparison in three calculations, for spherical (sp) and collective (c) states.

	PFSDG-U			MSCM			IM-SRG		
	E_x	$n^{\pi}_{p\text{-}h}$	$n^{\nu}_{p\text{-}h}$	E_x	$n^{\pi}_{p\text{-}h}$	$n^{\nu}_{p\text{-}h}$	E_x	$n^{\pi}_{p\text{-}h}$	$n^{\nu}_{p\text{-}h}$
0^+_{sp}	0.00	0.56	0.38	0.00	0.39	0.65	0.00	0.67	0.39
2^+_{sp}	3.15	1.47	1.55	2.57	0.91	1.67	3.25	0.85	1.34
4^+_{sp}	3.66	1.14	1.40	3.26	0.69	1.44	3.63	—	—
0^+_{c}	2.65	2.35	2.70	2.61	2.54	2.72	—	—	—
2^+_{c}	2.88	2.22	2.51	2.88	2.54	2.72	—	—	—
4^+_{c}	3.44	2.49	2.72	3.43	2.52	2.73	—	—	—

The unit of the excitation energy, E_x, of each state is MeV.

Reaction selectivity for collective states

This is still an open question:

- The spectroscopic factor for the $(p, 2p)$ and two-nucleon amplitude for the $(p, 3p)$ in the calculations prefers populating spherical states rather than deformed states.
- No theory for explaining the mechanism of the $(p, 3p)$ reaction is available.

Reaction selectivity for collective states

This is still an open question:

- The spectroscopic factor for the $(p, 2p)$ and two-nucleon amplitude for the $(p, 3p)$ in the calculations prefers populating spherical states rather than deformed states.
- No theory for explaining the mechanism of the $(p, 3p)$ reaction is available.

In a naive picture...

- In 1p knockout reaction, 1p-1h (particle-hole) may be favored.
- While, the final state of 2p removal reaction may be more connected to 2p-2h and more particle-hole excitations.

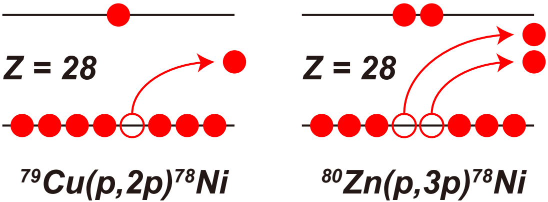

Low inclusive cross sections of ^{78}Ni

- The reaction cross sections (inclusive cross sections, σ_{incl}) were also investigated.
- The cross section to produce ^{78}Ni were found as almost 4 times lower than other isotones.

Reaction		σ_{incl} (mb)
^{79}Cu $\rightarrow$ ^{78}Ni	-1p	1.7(4)
^{80}Zn $\rightarrow$ ^{79}Cu	-1p	8.0(3)
^{81}Ga $\rightarrow$ ^{80}Zn	-1p	5.2(3)
^{82}Ge $\rightarrow$ ^{81}Ga	-1p	7.5(9)
^{80}Zn $\rightarrow$ ^{78}Ni	-2p	0.016(6)
^{81}Ga $\rightarrow$ ^{79}Cu	-2p	0.061(5)
^{82}Ge $\rightarrow$ ^{80}Zn	-2p	0.067(8)

Quasi-free $(p, 2p)$ reaction theory

- DWIA (distorted-wave impulse approximation) calculation (K.Ogata) for ^{79}Cu$(p, 2p)^{78}$Ni reaction[1].
- Reproduced well for the reaction cross section of neutron-rich oxygen isotopes with shell-model calculations with SFO interaction in p and sd shells[2].
- Product of spectroscopic factor C^2S from shell-model and single-particle cross section $\sigma_{\rm sp}$ as below:

$$\sigma_{\rm th}(j, \alpha) = C^2S(j, \alpha) \cdot \sigma_{\rm sp}(j, S(\alpha))$$

[1] T. Wakasa *et al.*, Prog. Part. Nucl. Phys. **96**, 31-87 (2017)
[2] S. Kawase *et al.*, Prog. Theor. Exp. Phys. **2018**, 021D01 (2018)

Most final states after the reaction may be unbound

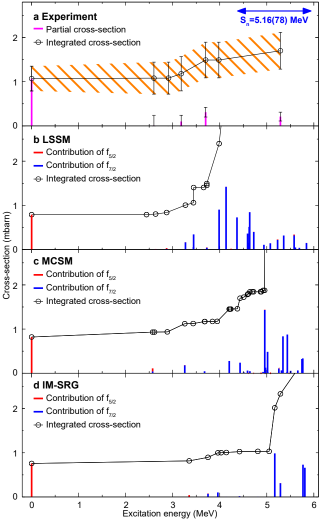

- Evolutions of running sum (black line) in experiment and theory are in consistent up to 5 MeV.
- Most strength above neutron separation energy S_n in MCSM.
- Confirmed the understanding of the $(p, 2p)$ reaction with the DWIA calculation

Table of Contents

Conclusion and outlook

Conclusion of this work

- Strong γ-ray transition at 2600(33) keV was confirmed as the first excitation state.
- The agreement with several calculations showed the doubly magic nature in ^{78}Ni
- A finding of second 2^+ state at 2910(43) keV in the $(p, 3p)$ reaction suggested the shape coexistence in ^{78}Ni

Conclusion and outlook

Conclusion of this work

- Strong γ-ray transition at 2600(33) keV was confirmed as the first excitation state.
- The agreement with several calculations showed the doubly magic nature in ^{78}Ni
- A finding of second 2^+ state at 2910(43) keV in the $(p, 3p)$ reaction suggested the shape coexistence in ^{78}Ni

Future outlook

- Spectroscopic measurement beyond ^{78}Ni is desired.
- To investigate the shape coexistence, the measurement of 0_2^+ state in ^{78}Ni should also be considered.
- The development of the understandings of the reaction mechanism for the $(p, 3p)$ is also desired.

Backup slides

Evolution of spectra with γ-ray multiplicity conditions

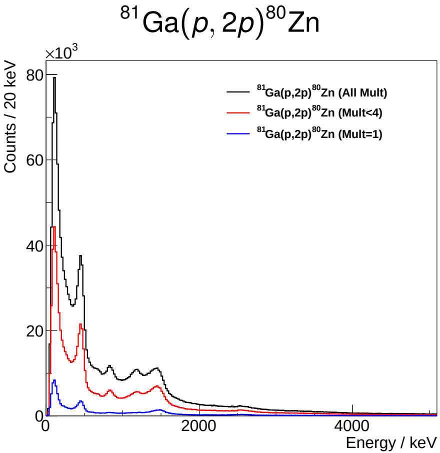

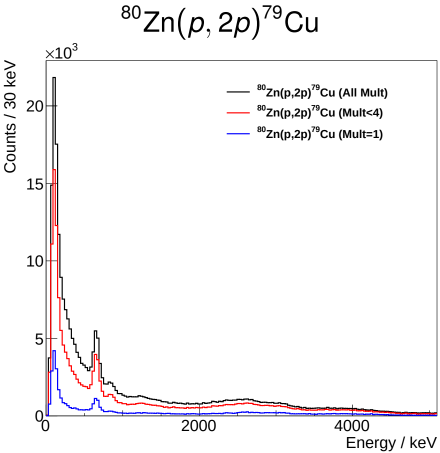

Evolution of spectra with time conditions of DALI2

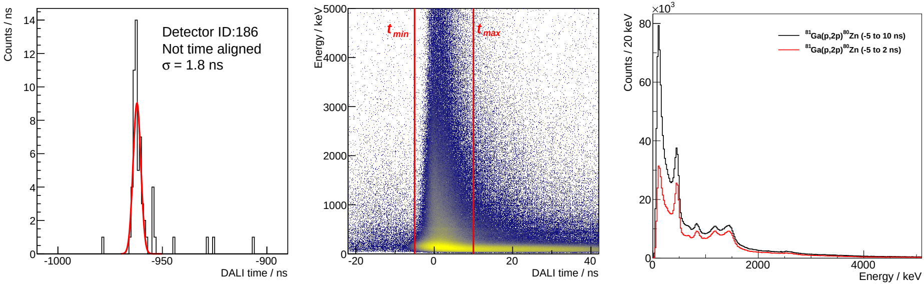

Simulated response function of DALI2

- The detector response was evaluated with GEANT4 Monte-Carlo simulation package
- Energy resolution for each scintillator was determined by soure measurements
- Calibration sources ^{60}Co, ^{88}Y, and ^{137}Cs
- Background events were fitted by double-exponential function

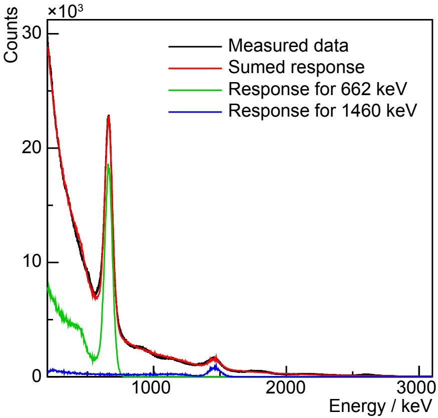

- Test case with source measurement with ^{137}Cs (662 keV)

Vertex reconstruction and target tichkness

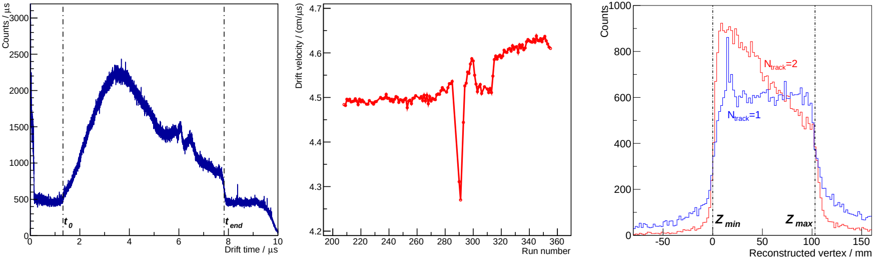

Calibration of γ-ray spectrometer